Contents lists available at ScienceDirect

Applied Catalysis B: Environmental

The role of water on the selective decarbonylation of 5-hydroxymethylfurfural over Pd/Al$_2$O$_3$ catalyst: Experimental and DFT studies

Qingwei Meng [a,b], Dongbo Cao [a,c], Guoyan Zhao [c], Chengwu Qiu [a,b], Xingchen Liu [b], Xiaodong Wen [a,c], Yulei Zhu [a,c,*], Yongwang Li [a,c]

[a] State Key Laboratory of Coal Conversion, Institute of Coal Chemistry, Chinese Academy of Sciences, Taiyuan 030001, PR China
[b] University of Chinese Academy of Sciences, Beijing 100049, PR China
[c] Synfuels China Company Ltd., Beijing 101407, PR China

ARTICLE INFO

ABSTRACT

Highly selective decarbonylation of 5-hydroxymethylfurfural (HMF) to furfuryl alcohol (FOL) was originally realized by adding water to organic solvent. Side reactions such as hydrogenolysis, dehydrogenation and etherification could be effectively suppressed by introducing appropriate amount of water in pure organic solvent. Based on DFT calculations, hydrogen bonds between hydroxymethyl groups and water hinder the dehydrogenation of FOL to furfural (FAL) and furan. On the other hand, in situ water-pyridine-FTIR measurements revealed that the hydrogen bonding interaction between water and the hydroxyl groups on γ-Al$_2$O$_3$ surface decrease the acidity of Pd/Al$_2$O$_3$ and suppresses side reactions such as hydrogenolysis and etherification. Therefore, adding water to organic solvent could be a strategy for the protection of hydroxyl groups.

1. Introduction

As an abundant carbon resource and an ideal replacement for fossil fuels, biomass has attracted more and more research and application attentions. Furfuryl alcohol (FOL) is an important biomass-derived chemical, and it can be used for the manufacture of resins, rubbers and fibres [1–3]. Presently, FOL is produced by hydrogenation of furfural (FAL) [4,5]. However, FOL can be produced alternatively by the decarbonylation of 5-hydroxymethylfurfural (HMF, from C6 sugar) due to the greater availability and versatility of C$_6$ than C$_5$ sugars in biomass feedstock.

It has been reported that homogeneous [IrCl(cod)]$_2$PCy$_3$ [6] and heterogeneous Pd/SBA-15 [7] catalysts catalyze the decarbonylation of HMF under inert atmosphere or air efficiently. However, the high costs and anhydrous operating conditions restrict the large-scale application of these catalysts. In comparison, Pd/Al$_2$O$_3$ is effective but less expensive for HMF decarbonylation

[8,9], although the acidic support could lead to dehydrogenation, hydrogenolysis etc. side reactions even under N$_2$ atmosphere [9]. We have increased the selectivity of FOL to 92% by suppressing the acidity of Pd/Al$_2$O$_3$ catalyst using alkali earth metal [8], but simple and operable method is desirable. Water, with Lewis base character, has been reported to have a detrimental effect on Lewis acid reactivity [10], which may thus influence the decarbonylation selectivity. In fact, water is produced in the process of HMF production, or the hydrolysis of cellulose to hexose and the dehydration of hexose to HMF. Therefore, it would be advantageous to achieve transformation of HMF in the presence of water.

Solvent effect is an important issue for liquid phase reactions. As the most important green solvent, water could also serve as a reaction promoter. Compared with many other organic solvents, its remarkable superiority could be its great ability to form hydrogen bond, which has been demonstrated in homogeneous catalysis systems [11–13]. At the interface of the aqueous and organic phases, water is supposed to interact with the organic substrates through hydrogen bond and promote their activity accordingly. This has been demonstrated by computer simulations that hydrogen bonds between water molecules and hydrogen-bond accepting groups in the complex could lower the energy of activation for Diels-Alder reaction [14]. The solvent effect of water in heterogeneous catalysts

has also been reported in a few publications [15,16]. The activity of hydrogenation of acetophenone to 1-phenylethanol was promoted significantly when water was used as the solvent over Rh/Al$_2$O$_3$ and Rh/C [15]. This was achieved by the interactions between the carbonyl groups of substrates and water through hydrogen bonds on Rh/C, and the hydrogen bonds between water and the hydroxyl groups on the catalyst surfaces of Rh/Al$_2$O$_3$. Water is also useful as effective multiphase reaction media for modification of selectivity. For example, the *n*-hexane-CO$_2$-water medium promoted the selectivity for the hydrogenation of benzyl cyanide to 2-phenylethylamine over Pd/Al$_2$O$_3$ [16]. However, the hydrogen-bonding functional mechanism of water and the solvation effect has not been investigated in detail in heterogeneous catalysis, where solid-liquid interfaces exist.

Herein, a combined and water-containing solvent system is originally reported for the selective decarbonylation of HMF using a Pd/Al$_2$O$_3$ catalyst, and the selectivity of FOL is increased significantly to 97% with a water content of 28 wt%. The functional mechanism of water is carefully explored by the help of DFT and in situ water-pyridine-FTIR with the solvation effect considered. It is proved that the hydrogen bonding interaction between water and hydroxyl in FOL inhibits the hydroxymethyl group from dehydrogenation side reaction. Moreover, the water, with Lewis base character, could coordinate onto Lewis acid sites of γ-Al$_2$O$_3$, decrease the acidity of Pd/Al$_2$O$_3$ and suppress side reactions such as hydrogenolysis and etherification.

2. Experimental section

2.1. Catalyst preparation and evaluation

Pd/Al$_2$O$_3$ and Pd/Al$_2$O$_3$-AlOOH with 1 wt% of nominal Pd loading were prepared using an incipient wetness impregnation method. Firstly, Al$_2$O$_3$ (Aluminum Co., Ltd, of China) or Al$_2$O$_3$-AlOOH powders were impregnated with calculated amount of Pd(NO$_3$)$_2$ (Sinopharm Chemical Reagent Co., Ltd) aqueous solution containing 10 mg/mL of Pd for 5 h, followed by drying at 80 °C for 16 h and calcinating at 400 °C for 2 h. Prior to the reactions, the catalysts were reduced off-line with an H$_2$ flow at 250 °C for 2 h. The tests were performed in a 50 mL stainless steel autoclave with an inserted Teflon vessel. Typically, 1.2 g HMF (Shang Hai DEMO Medical Tech. Co., Ltd, China), 25 g solvent and 0.12 g catalysts were introduced into the autoclave. Afterwards, the reactor was purged with H$_2$ for several times to remove the air, and then heated to 180 °C. After the reactions are complete, the autoclave was cooled down rapidly by ice-water bath. The tail gas was collected and analyzed off-line by two gas chromatographs (models 6890N, Agilent, USA) equipped with a FID and a TCD detector respectively. The furan-derived compounds in the gaseous phase were less than 1% (mol) and could be neglected. The liquid products were filtered to remove the solid catalysts and were analyzed by another gas chromatograph (models 6890N, Agilent, USA) equipped with a DB-WAXETR capillary column (30 m × 0.32 mm × 0.5 um). The conversion and the selectivity were determined by the area normalization method. The content of FOL and HMF were also tested by external standard method normalized by the area of the solvent. The results calculated by the two methods were consistent. The conversion and selectivity of products for the reactions were calculated based on the following equations (Note: the actual selectivity of difurfuryl ether is two times of the calculated value from the equation below):

$$\text{Conversion}\,(\%) = 100 - \frac{\text{Amount of HMF after reaction (mol)}}{\text{Total amount of HMF (mol)}} \times 100$$

$$\text{Selectivity}\,(\%) = \frac{\text{Amount of a product (mol)}}{\text{Total amount of HMF converted (mol)}} \times 100$$

2.2. Catalyst characterization

The influence of water on the acidity of the catalyst was examined by the in situ FTIR measurements using a VERTEX70 Bruker FTIR Spectrometer. Typically, the catalyst was reduced in situ with flowing H$_2$ at 250 °C for 2 h prior to the measurement. Then the sample was degassed in vacuum (1 × 10^{-2} Pa) at 300 °C for 30 min and then cooled to 30 °C. After that, the catalyst was exposed to the water vapor for 30 min, repeating for several times. Finally, the sample was exposed to pyridine for 30 min. The spectra were recorded at 30 °C, 150 °C and 300 °C after vacuuming for 30 min.

2.3. Methods and models for DFT calculations

The plane-wave DFT calculations were carried out using the Vienna ab initio simulation package (VASP), version 5.3 [17,18]. The electron-ion interaction was described with the projector augmented wave (PAW) method [19,20]. The generalized gradient approximation and the Perdew-Burke-Ernzerhof functional (GGA-PBE) [21] were used to describe the exchange and correlation energies for all systems, and considering the long-range dispersion correction PBE-D3 functional for vdW interaction [22–24]. In the computations, an energy cutoff of 400 eV was chosen for the plane-wave basis set.

A 4 × 4 Pd(111) surface with a thickness of four atom layers was employed for all calculations. The bottom two layers were frozen, and the top two layers were allowed to relax. The vacuum layer between periodically repeated slabs was set as 20 Å to avoid interactions among slabs. The Brillouin zone was sampled with a 3 × 3 × 1 k-point grid. Surface relaxation was performed until all forces were smaller than 0.05 eV/Å. To locate the transition states of decarbonylation of HMF on Pd(111), the nudged elastic band (NEB) method [25] was applied and the stretching frequencies were analyzed to characterize transition state with only one imaginary frequency.

The adsorption energy was defined as E$_{ads}$ = E$_{slab+i}$ − E$_{slab}$ − E$_i$, where E$_{slab+i}$ is the total energy of the adsorbate/slab system, E$_{slab}$ is the total energy of the clear slab and E$_i$ is the total energy of the adsorbate in gas phase. The reaction barrier (E$_a$) and reaction energy (E$_r$) are defined as E$_a$ = E$_{TS}$ − E$_{IS}$ and E$_r$ = E$_{FS}$ − E$_{IS}$, where E$_{IS}$, E$_{TS}$, and E$_{FS}$ are the energies of the corresponding initial state (IS), transition state (TS) and the final state (FS).

The solvation energy and solvation effect on reaction energy and barrier are calculated with VASPsol software [26].

3. Results and discussion

3.1. Decarbonylation performance of HMF over Pd/Al$_2$O$_3$ catalyst in different media

Decarbonylation of HMF was studied with Pd/Al$_2$O$_3$ catalyst in different reaction media at 180 °C. Under these conditions, a series of products were produced, including desired product FOL; side products: FAL and furan, 2-methylfuran (2-MF), 2, 5-dimethylfuran (DMF) and 5-methylfurfural (MFAL), and etherification products. The reaction pathways of the products are shown in Scheme 1 as previously reported [9]. The sources of side products fall into three categories: hydrogenolysis, dehydrogenation and etherification reactions. In the solvent of 1, 4-dioxane, difurfuryl ether (DFE) was the main etherification product. When methanol or ethanol was added into 1, 4-dioxane, large amount of ether 5-methoxymethylfurfuryl alcohol (MOMFOL) or 5-ethoxymethylfurfuryl alcohol (EOMFOL) appeared. MOMFOL and EOMFOL are likely produced respectively by etherification of
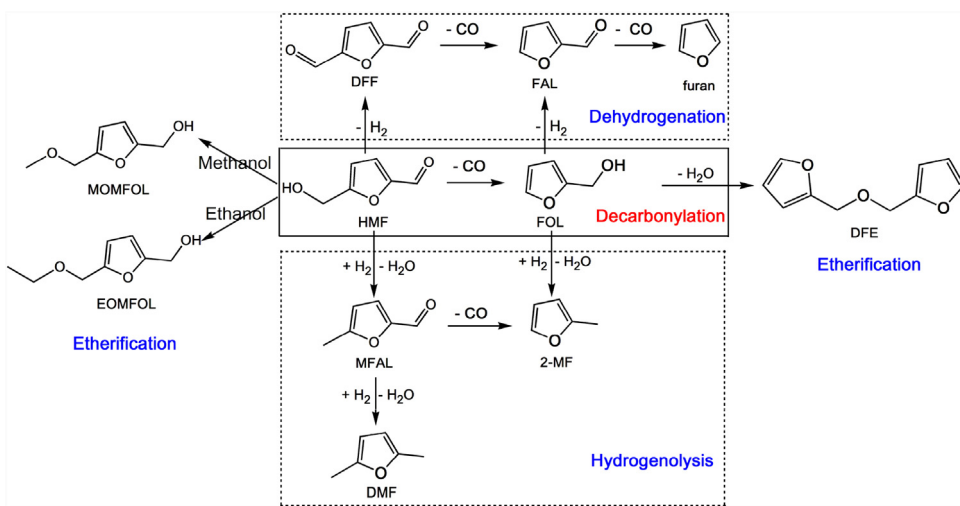
Scheme 1. The reaction pathways in decarbonylation of HMF.

methanol/ethanol and 2, 5-dihydroxymethylfuran (DHMF), which was formed by aldehyde hydrogenation of HMF. It can be observed that, all the side products are derived from the evolution of the furan ring-branched hydroxymethyl, which occurs via hydrogenolysis, dehydrogenation and etherification reactions. However, the product distribution is significantly different with different reaction media.

Table 1 shows the catalytic performance of Pd/Al$_2$O$_3$ in different reaction media. 1, 4-dioxane was selected as the parent solvent, as HMF exhibits fantastic stability in this solvent [6,7]. The reaction was also conducted in several other organic solvents (see Table S1) and 1, 4-dioxane enables the highest FOL yield. But significant hydrogenolysis and dehydrogenation as well as some etherification products were produced in the pure 1, 4-dioxane, leading to a low selectivity of FOL (Table 1 entry 1). However, after water was introduced into the 1, 4-dioxane, the yield of by-products showed an opposite trend with the contents of added water (Table 1 entry 2–4). When 28% of water was added, the selectivity of FOL reached 97%, indicating that side reactions have been suppressed significantly. But large amount of water (40%) led to decreased conversion and increased dehydrogenation/polymerization reactions. Water could enhance polymerization or degradation of biomass due to its special nature of furan ring. While furfural may be the intermediate from HMF to polymers as water could promote condensation and resinification etc. side reactions of furfural [27]. The increased furfural selectivity in 40 wt% water solvent further verifies this assumption. Furthermore, serious polymerization occurred when pure water was used. The reaction time was prolonged to 16 h and gas exchange was conducted in the middle of reaction in the media of 28% water. As a result, a total conversion was achieved and a FOL yield of 95% was obtained. Removal of water by molecular sieve has been reported to be necessary for decarbonylation of HMF over Pd/SBA-15 under air atmosphere [7] and for sequential dehydration and decarbonylation of fructose over homogeneous Pd(OAc)$_2$ under N$_2$ atmosphere [28]. The contradictory results in this work were probably caused by the different support and the reaction atmosphere. As the decarbonylation of HMF over Pd/Al$_2$O$_3$ catalyst has been successfully achieved in water under vacuum [29]. Furthermore, the isopropanol (80 wt%)–water (20 wt%) mixture has been reported to promote the selective decarbonylation of FAL over Pd/Al$_2$O$_3$, in which isopropanol could decompose to hydrogen [30]. The presence of water in crude HMF is inevitable as HMF is produced by dehydration of hexose. Furthermore, aqueous-organic bi-phase system has been used to convert carbohydrates to HMF [31–35]. This work demonstrates that proper content of water

in the organic solvent is favorable to the selective decarbonylation. Hence, the removal of water after the production of HMF and prior to the decarbonylation could be omitted or simplified.

To explore the mechanism of this solvent effect, methanol and ethanol were added into pure 1, 4-dioxane (Table 1 entry 7–8). When 28 wt% of methanol or ethanol was used, the hydrogenolysis and dehydrogenation side reactions were also weakened. However, the high amount of MOMFOL and EOMFOL ethers in the two solvents led to no significant increase of FOL selectivity. H$_2$ solubility in the solvent is generally an important factor influencing the hydrogenolysis selectivity. Although the H$_2$ solubility in ethanol is higher than that in 1, 4-dioxane [15], the hydrogenolysis in 28 wt% of ethanol is weaker than that in pure 1, 4-dioxane. Furthermore, the H$_2$ solubility cannot explain the suppression of dehydrogenation and etherification reactions by the added co-solvent. Comparing Table 1 entry 1, 4, 7, 8, we could find that the hydrogenolysis and dehydrogenation products are gradually suppressed with the co-solvent order: ethanol < methanol < water, which corresponds to the hydrogen-bond-donation capability of the three protic solvents [15]. The hydrogen bonds between the protic solvent and Rh/Al$_2$O$_3$ or the substrates have been reported to influence the catalytic performance. In addition, hydrogen bonding interactions could be formed between protic solvents and the hydroxyl groups on Al$_2$O$_3$ surfaces [15] as well as on the active hydroxymethyl groups of HMF or FOL. As all the side reactions occur on the furan ring-branched hydroxymethyl group, the hydrogen bonding of water on hydroxyl of HMF or FOL may change the reaction barrier of the side reactions. Meanwhile, the hydrogen bonding of water on the hydroxyl groups of Al$_2$O$_3$ surfaces may change the acidity of the catalyst, which could influence the activity of etherification and hydrogenolysis side reactions [8]. The effect of these hydrogen bonding interactions were further explored below.

3.2. Hydrogen bonds between hydroxyls in FOL and water

To verify the mechanism of hydrogen bonds in this work, reactions on substrates with different groups: hydroxyl (FOL), carbonyl (FAL) and methyl (2-MF) group were also conducted (Table 2). As the hydrogen bond acceptance ability of the hydroxyl (in FOL) is higher than that of aldehyde group (in FAL) and methyl (in 2-MF), different suppression extent of reactions on these groups is expected. The hydroxymethyl in FOL goes through hydrogenolysis, dehydrogenation and etherification reactions in pure 1, 4-dioxane, producing 2-MF, FAL/furan and DFE respectively. In the system with 28% water, these reactions are almost suppressed completely,

Table 1
Decarbonylation of HMF over Pd/Al$_2$O$_3$ in different solvents.[a]

Entry	Solvent	Conv.	Selectivity (%)				
			FOL	Hydrogenolysis2-MF + DMF + MFAL	DehydrogenationFuran + FAL	ethers	Others[f]
1	1, 4-dioxane	63.8	72.7	14.7	7.6	3.4[c]	1.6
2	12% water	63.7	90.7	2.7	1.8	2.0[c]	2.8
3	20% water	63.2	96.1	1.3	1.4	1.2[c]	–
4	28% water	62.1	97.3	0.5	–	0.5[c]	1.7
5	40% water	53.0	73.3	0.7	11.1	2.5[c]	12.4
6[b]	**28% water**	**100**	**95.3**	**2.9**	**1.6**	**–**	**0.2**
7	28%methanol	95.7	75.3	6.3	1.5	15.9[d]	1
8	28%ethanol	98.7	64.3	9.5	3.9	22.3[e]	–

[a] Conditions: 25 g Solvent: water/methanol/ethanol in 1, 4-dioxane (weight ratio), 1.2 g HMF, 0.12 g Pd/Al$_2$O$_3$, H$_2$: atmospheric pressure (room temperature), 180 °C, 6 h.
[b] Reaction for 8 h, cooling down and purging with fresh H$_2$, reaction for another 8 h.
[c] DFE.
[d] MOMFOL.
[e] EOMFOL.
[f] Others mainly include ring-opening products and polymers. FOL = furfuryl alcohol, 2-MF = 2-methylfuran, DMF = 2,5-dimethylfuran, MFAL = 5-methylfurfural, FAL = furfural, DFE = difurfuryl ether, MOMFOL = 5-methoxymethylfurfuryl alcohol, EOMFOL = 5-ethoxymethylfurfuryl alcohol.

Table 2
The effect of solvents on conversion of FOL and FAL.[a]

Substrate	Solvent	Conv. (%)	Yield (%)				
			Furan	2-MF	FAL	FOL	ether[b]
FOL	1,4-dioxane	36.2	3.1	17.9	3.8	–	11.4
	28% water	3.3	0.5	1.5	0.6	–	0.7
FAL	1,4-dioxane	22.0	13.5	0.7	–	7.9	–
	28% water	20.1	16.9	0	–	3.3	–
2-MF	1,4-dioxane	trace					
	28% water	trace					

[a] Conditions: 25 g Solvent: water in 1, 4-dioxane (weight ratio), 1.2 g substrate, 0.12 g Pd/Al$_2$O$_3$, H$_2$: atmospheric pressure, 180 °C, 6 h.
[b] DFE.

which is consistent with the reaction results of HMF in Table 1. Besides decarbonylation, hydrogenation of the carbonyl group in FAL occurs, forming FOL. In the solvent with 28% water, only approximately half of the hydrogenation product FOL is suppressed. This means that the stability of the groups by water is in line with the hydrogen bond acceptance ability (–CH$_2$OH > –CHO), which verifies the presence of the hydrogen bonding interactions between water and the hydroxyls of FOL and HMF. The weaker effect of water on FAL decarbonylation than that on HMF decarbonylation further verifies that the hydrogen bonds between water and hydroxymethyl groups work in the decarbonylation process of HMF. 2-MF exhibits trace conversion in both solvents. The functional mechanism of the hydrogen bonds between water and the hydroxyls of FOL or HMF and the solvation effect was investigated via DFT calculations below.

3.2.1. DFT calculations for the hydrogen bonds between water and hydroxyls in FOL

To probe the effect of the hydrogen bond, the reaction mechanism of HMF was investigated first to determine the proper chemical model. The calculations were conducted on the close-packed Pd(111) surfaces. The HRTEM histogram of the reduced Pd/Al$_2$O$_3$ (see Fig. S1) also confirms the preferentially exposed Pd(111) faces. As decarbonylation, dehydrogenation and hydrogenolysis reactions need metallic Pd sites in the experiments, DFT calculations were employed to study the mechanism of these three reactions on Pd(111). To start with, the adsorption modes were explored and the most stable molecular adsorption structure of HMF((CH$_2$OH)C$_4$H$_2$(CHO)O*), DFF(C$_4$H$_2$(CHO)$_2$O*), and FOL(C$_4$H$_3$(CH$_2$OH)O*) are shown in Fig. 1 and Table 3.

HMF adsorbs over the fcc-hollow site and oxygen over the bridge site in a planar arrangement with the adsorption energy of −1.40 eV, which is stronger than that bent adsorption on Co$_3$O$_2$/Pt(111) surface with −0.8 eV [36]. In the structure of adsorbed HMF, the furan ring is bonded with the surface Pd atoms with four bonds, and O atom is located over the bridge site. The C—C bonds between the C atoms of furan ring and those of ligands of CHO and CH$_2$OH are both activated with 1.460 and 1.532 Å, respectively, while those bonds of HMF molecular are 1.441 and 1.494 Å (see Table 3). Due to low H$_2$ pressure in the experiments of HMF reactions and the adsorption energy of hydrogen on Pd(111) at 0.25 and 0.50 ML (−0.67 and −0.64 eV), the adsorption of HMF is much stronger than that of H atoms [37]. Thus, the most stable configurations of HMF cannot be affected by the H atoms. For solvent molecules, the H$_2$O adsorption energies on Pd(111) of isolated monomer and octamer are −0.22 and −0.60 eV, respectively [38]. The adsorption energy of 1,4-dioxane on Pd(111) is positive, which indicates 1,4-dioxane cannot be chemisorbed on Pd(111). Therefore, the adsorption of solvent molecules cannot affect the most stable configurations of HMF.

FOL and 2, 5-diformylfuran (DFF) are both adsorbed with the furan ring centered over the hollow sites. The adsorption energies are −1.46 and −1.79 eV, respectively. The FOL structure is in a very close agreement with the DFT calculations by Vorotnikov et al., though the adsorption energy they found is higher by 0.53 eV, possibly due to the different methods [39]. For the adsorbed HMF, FOL, and DFF, the adsorption energy of DFF is the strongest, because the ligands of CH$_2$OH are farther away from the surface than the ligands of CHO. These structures are consistent with that determined by high-resolution electron energy loss spectroscopy (HREELS) and temperature-programmed desorption (TPD) to study the adsorption and thermal chemistry of 2, 3-dihydrofuran (2, 3-DHF) and 2, 5-dihydrofuran (2,5-DHF) on Pd(111) confirming that the π electrons within the olefin functions in the furan ring and carbonyl interact more strongly with the surface than lone pairs in oxygen atoms. In the structure of adsorbed FOL, the C—C bond between the C atom of furan ring and that of hydroxymethyl ligand is lengthened with 1.530 Å, while the bond of FOL molecular is 1.493 Å. In the structure of adsorbed DFF, the C—C bonds between the C atoms of furan ring and those of ligands of CHO are activated slightly with 1.446 and 1.454 Å, respectively, while the bonds of DFF molecular is 1.446 Å (see Table 3).

The reactions mechanism of HMF is investigated using DFT methods and the potential energy diagram is shown in Fig. 2 (decarbonylation reaction in black line, dehydrogenation in red line and hydrogenolysis in blue line). The structures of reactants, products, intermediates, and the transition states are shown in Fig. S2. The first elementary step for all the three reactions is dehydrogenation. One is the dehydrogenation reaction of the hydroxymethyl ligand to form (CH$_2$O)C$_4$H$_2$(CHO)O*, followed by hydrogenolysis reaction
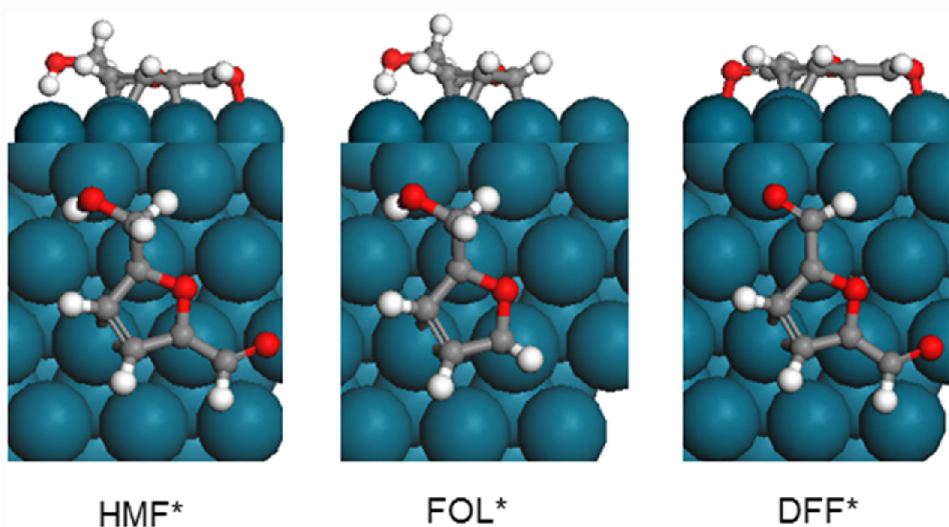
Fig. 1. The structures for the most stable molecular adsorption mode for HMF ((CH$_2$OH)C$_4$H$_2$(CHO)O*), FOL ((CH$_2$OH)C$_4$H$_2$O*), DFF (C$_4$H$_2$(CHO)$_2$O*).

Table 3
Properties of HMF, DFF, and FOL adsorption on Pd(111). (d$_{Pd-\alpha C}$, the carbon atom closest to the oxygen; d$_{Pd-\beta C}$, the carbon atom farthest from the oxygen).

|	d$_{Pd-\alpha C}$ (Å)	d$_{Pd-\beta C}$ (Å)	d$_{Pd-O}$ (Å)	d$_{C-C}$ (Å)	ΔE_{ads} (eV)
HMF	2.097/2.132	2.232/2.240	2.150	1.460/1.532	−1.40
FOL	2.066/2.092	2.215/2.241	–	1.530	−1.46
DFF	2.155/2.161	2.246/2.289	2.084/2.104	1.446/1.454	−1.79
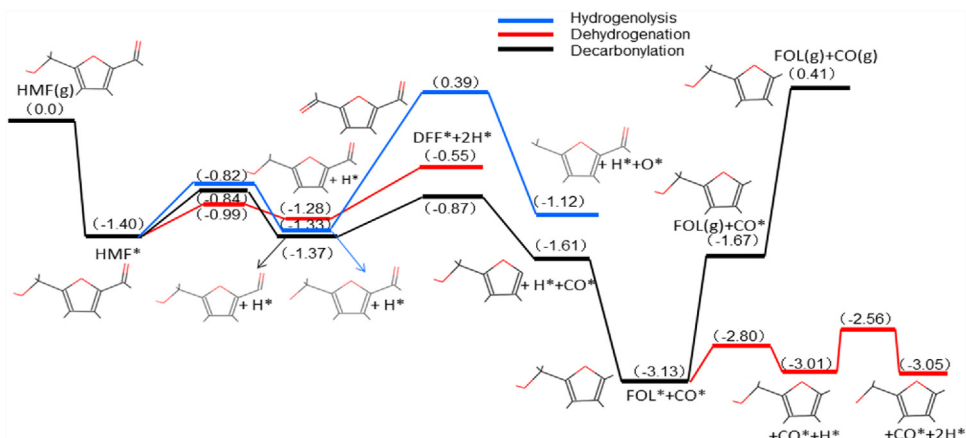
Fig. 2. Potential energy diagram for the decarbonylation reactions of HMF on Pd(111); Energies in eV are relative to gas phase HMF plus the clean slab.

to form 5-methylfurfural (MFAL). This step needs an energy barrier of 0.58 eV, and is endothermic with 0.07 eV (the blue line). The other pathway is the loss of aldehydic hydrogen, which is endothermic by 0.03 eV with the energy barrier of 0.56 eV (the black line). The third path is the dehydrogenation reaction of the hydroxymethyl ligand to form (CHOH)C$_4$H$_2$(CHO)O*, which is slightly endothermic by 0.12 eV and has an energy barrier of 0.41 eV (the red line). At the second step, the hydrogenolysis reaction of (CH$_2$O)C$_4$H$_2$(CHO)O* to form (CH$_2$)C$_4$H$_2$(CHO)O* has a very high energy barrier of 1.72 eV, and is endothermic with 0.21 eV. The second step of the dehydrogenation reaction that removes H atom on CHOH ligand to form DFF is strongly endothermic by 0.73 eV with no barrier. However, the decarbonylation reaction of intermediate is exothermic by 0.24 eV with an energy barrier of 0.50 eV. Then, the hydrogenation of the produced (CH$_2$OH)C$_4$H$_2$O* intermediate to form FOL is strongly exothermic by 1.52 eV with no energy barrier (the black line). For comparison, FOL is preferred to form thermodynamically, since

DFF formation via dehydrogenation reaction is highly endothermic reaction, while the hydrogenolysis reaction needs the high barrier. FOL and CO desorption needs 1.46 and 2.08 eV, respectively. The calculation results are in agreement with the experimental results displayed in Table 1, as FOL is the main product by decarbonylation of HMF. Thus, the main dehydrogenation side product FAL, the sequential decarbonylation product furan and the hydrogenolysis side product 2-MF are mainly derived from FOL. Therefore, the effect of hydrogen bond between water and hydroxymethyl in FOL is explored by DFT calculations.

Vorotnikov et al. [39] have studied the mechanism of elementary steps and found that the dehydrogenation of FOL to FAL and sequential decarbonylation to form furan were strongly exothermic with 0.56 eV and 1.46 eV respectively, while the hydrogenolysis of FOL to form 2-MF was slightly exothermic with 0.07 eV. Our work also showed that the deoxygenation step in hydrogenolysis reaction of HMF needs high energy barrier. As a result, the formation of

Table 4
The reaction energies and energy barriers of the elementary reactions in dehydrogenation of FOL.

Reaction	Energy barrier (eV)		Reaction energy (eV)	
	No water	With water	No water	With water
$FOL^* \rightarrow (CHOH)C_4H_2O^* + H^*$	0.33	0.72/0.72[*]	0.12	0.30/0.32[*]
$(CHOH)C_4H_2O^* \rightarrow FAL^* + H^*$	0.45	0.67	−0.04	0.23

[*] With solvation effect considered.

Table 5
The solvation energies for HMF, FAL, MF, and FOL on Pd(111) in different solvents (water, methanol, ethanol and 1,4-dioxane).

	E_{sol} (eV)			
	water	methanol	ethanol	1, 4-dioxane
HMF	−0.66	−0.74	−0.50	−0.37
FOL	−0.61	−0.53	−0.58	−0.35
FAL	−0.22	−0.16	−0.13	0.06
2-MF	−0.14	−0.08	−0.06	0.11

FAL and furan from FOL is thermodynamically favored. In this work, it is found that the presence of water influences the products distribution due to the 1.666 Å hydrogen bond between hydroxymethyl of FOL and H_2O, and the effect of water on the dehydrogenation of FOL to FAL was investigated. The reaction energies and energy barriers for the elementary reactions of the dehydrogenation of FOL to form FAL are summarized in Table 4. The structure of FOL, intermediates, and the transition states are shown in Fig. S3.

For the first dehydrogenation step of FOL, the energy barrier is 0.33 eV, which is close to Vorotnikov et al.'s calculations (0.51 eV) [39]. For comparison, the energy barrier and reaction energy are increased by 0.39 and 0.18 eV respectively when hydrogen bonds exist between H_2O and the $-CH_2-OH$ groups of FOL. For the further dehydrogenation step of $(CHOH)C_4H_2O^*$ to FAL, the energy barrier is 0.45 eV, close to Vorotnikov et al.'s calculations (0.40 eV) [39]. Similarly, the energy barrier and reaction energy are also increased by 0.22 and 0.27 eV respectively in the presence of hydrogen bonding interactions of water. This indicates that the hydrogen bonds hinder the further dehydrogenation of FOL to FAL, which is consistent with the experiment results that the selectivity of FAL and furan was gradually decreased with rising content of water.

3.2.2. Solvation effect

To investigate the mechanism of the solvation effect, we used solvation theory to simulate the interaction between solute and the solvent. The solvation theory considers the electrostatic interaction between the solute and the solvent in polar or ionic systems, and the van der Walls interaction between nonpolar solutes and solvents, as well as the energy required to form a cavity in the solvent for large molecule systems. The solvation energy is calculated by the implicit solvation model which places a quantum-mechanical solute in a cavity surrounded by a continuum dielectric description of the solvent [26].

The solvation energies for HMF, FOL, FAL, and 2-MF on Pd(111) in the solvent of 1,4-doixane, water, methanol, and ethanol is shown in Table 5. For HMF, the solvent energy in the methanol solvent is the highest with −0.74 eV and then in water with −0.66 eV, while that in the 1,4-dioxane solvent is the lowest by −0.37 eV. For FOL, FAL and 2-MF, the solvent energy in water solvent is the highest, while that in the 1,4-dioxane solvent is the lowest. This suggests the water solvent affects the stability of these species strongly and enhances the adsorption of these species. Meanwhile, the water solvation energies for the hydroxyl group-containing species (HMF and FOL) are higher than those for carbonyl (FAL) or methyl (2-MF) group-containing species. As a result, the water solvation effect for HMF and FOL is stronger than that for FAL and 2-MF. This is consistent with the experimental results in Tables 1 and 2 that the water solvent affects the reactions on hydroxyl groups of HMF and FOL more remarkably than the reaction on the carbonyl group in FAL.

Furthermore, we investigated the water solvation effect on the first dehydrogenation step of FOL. The energy barrier and reaction energy with solvation effect considered are 0.72 and 0.32 eV. For comparison, the energy barrier and reaction energy of FOL dehydrogenation with one H_2O molecule on Pd(111) are 0.72 and 0.30 eV, similar with those in the water solvent. Therefore, the water solvent hinders the FOL dehydrogenation.

Though the calculations indicate that hydrogenolysis reactions of HMF and FOL are thermodynamically unfavored on Pd(111), higher amount of hydrogenolysis side products than dehydrogenation products were produced in pure 1, 4-dioxane in the experiments. This probably because that the hydrogenolysis reactions mainly follow the metal-acid synergistic mechanism, as is generally considered [40–43], by which the acid sites are responsible for the first dehydration step while the metallic sites are active phase for the next hydrogenation step. However, the DFT calculations were conducted on Pd (111). Thus, the acid sites are the major factor influencing hydrogenolysis activity in the experiments in this paper. The hydrogen bonding interactions between water and the hydroxyl groups on Al_2O_3 surfaces may influence the acidity of the Pd/Al_2O_3 catalyst, which will be discussed later.

Note that these calculations were conducted at relatively low coverage, thus, do not fully reflect the diverse species simultaneously present on the surface during reaction after large exposures.

3.3. Hydrogen bonds between hydroxyls on Al_2O_3 surfaces and water

The XRD patterns of Pd/Al_2O_3 catalyst at different reaction period in solvent of 28% water are given in Fig. S4. Two main peaks appear in all samples at 45.8° and 67° according to (400) and (440) crystal planes of the defective spinel structure respectively [44], indicating the stabilized structure of Al_2O_3 during reaction. The surface of the γ-Al_2O_3 is known to be in rich of hydroxyl groups [44], which could interact with water through hydrogen bonds [15]. The hydrogenolysis reactions may follow the metal-acid synergistic mechanism as is widely known [40–43,45], while the acid sites are also responsible for the active phase of etherification reaction [46,47]. Moreover, we have determined that, the hydrogenolysis and etherification side reactions in process of HMF decarbonylation were suppressed significantly when the acidity of Pd/Al_2O_3 decreases [8]. Therefore, the hydrogen bonding effect of water on the acidity of the catalyst is necessarily explored.

In situ water-pyridine-FTIR was designed to examine the effect of water on the acidity of the catalyst, as the concentration of acid sites could be probed by adsorption of pyridine. Prior to the adsorption of pyridine, water was adsorbed on the reduced Pd/Al_2O_3 for different times. The results at higher evacuation temperature after adsorption of pyridine correspond to stronger acidity of the catalysts. No evidence of a band at 1540 cm^{-1} was found in all the spectra, revealing no Brønsted acid sites capable of protonating pyridine on the alumina (Fig. S5) [48,49]. The characteristic peak of Lewis acid at 1450 cm^{-1}, was observed in all the spectra (Fig.
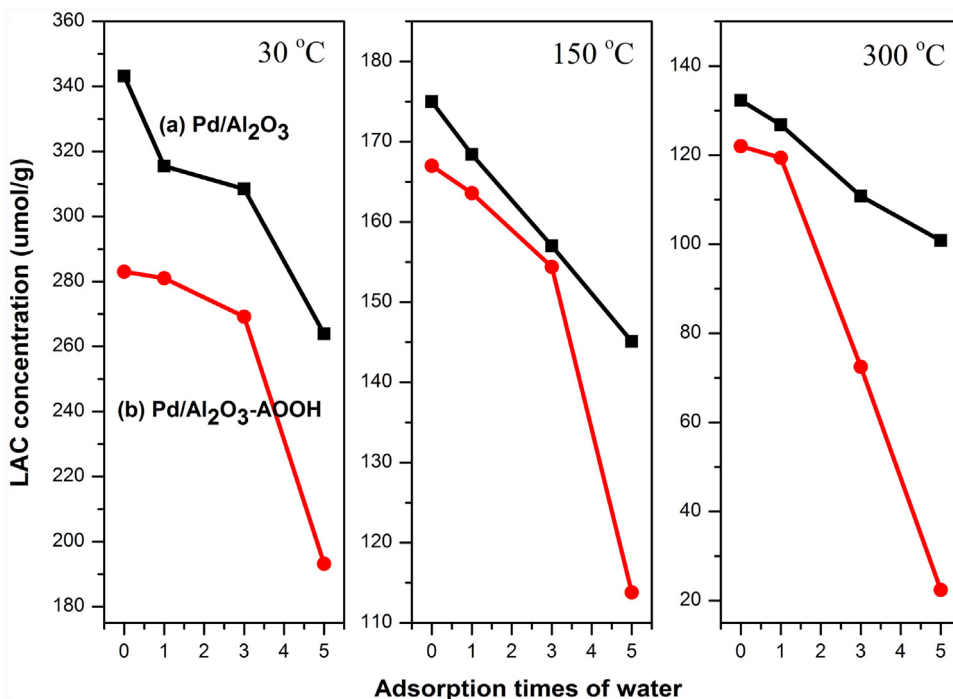
Fig. 3. Changes in Lewis acid site (LAS) concentration of (a) Pd/Al_2O_3 and (b) Pd/Al_2O_3-AlOOH as a function of adsorption times of water measured by adsorbed pyridine evacuation at different temperature.

S5). The concentration of Lewis acid sites (LAS) as a function of adsorption times of water is depicted in Fig. 3(a). It is obvious that the LAS concentration decreases significantly with the increasing adsorption times of water, indicating the decreased acidity of the Pd/Al_2O_3 catalyst by water.

To explore the mechanism of water influencing catalyst acidity, we compared the Pyridine-IR results of Pd/Al_2O_3 with that of another catalyst Pd/Al_2O_3-AlOOH. The Al_2O_3-AlOOH was formed by incomplete conversion of pseudoboehmite (γ-AlOOH) to Al_2O_3 via heat treatment, which actually is mixed structure of Al_2O_3 and AlOOH. Thus, Pd/Al_2O_3-AlOOH catalyst exhibits more surface hydroxyls as pseudoboehmite contains interlayer hydroxyl groups. If it is the hydrogen bond between water and the hydroxyl group on catalyst surface that led to the decrease of catalyst acidity, the loss speed of catalyst acidity would be related with the amount of surface hydroxyl groups. The XRD patterns of these two catalysts are displayed in Fig. S6(A). The FTIR spectra (see Fig. S6(B)) confirm that more hydroxyl groups are present in the structure of Pd/Al_2O_3-AlOOH. Moreover, the water-pyridine-FTIR results (Fig. 3(b)) show that the LAS concentration of Pd/Al_2O_3-AlOOH is lower than that of Pd/Al_2O_3 and is decreased more sharply with increasing adsorption times of water. This reveals that the increasing hydroxyl groups on catalyst surface could facilitate the adsorption of water, leading to notably reduced catalyst acidity.

The LAS are formed by coordinatively unsaturated species [50] and generally associated with tetrahedrally coordinated Al atoms, although desorption of nonbridging terminal hydroxyl groups on octahedrally coordinated Al may also generates LAS [51]. Thus the decrease of the LAS concentration is due to the reduced amount of coordinatively unsaturated Al species. It has been reported that the catalytic turnovers on LAS were inhibited by solvent molecules with Lewis base character, for example water [52–54] or the water–organic mixtures [55–57] used typically in biomass utilization process, through coordination on to the LAS [10,58]. Moreover, such bonding becomes stronger upon concurrent hydrogen bonding interactions with proximal hydroxyl groups [53]. The

competitive binding of molecular water onto LAS in γ-Al_2O_3 is evident due to the highly exothermic adsorption enthalpies [44]. Thus, it is deduced that the decrease of acidity of Pd/Al_2O_3 is due to the coordination of molecular water onto the LAS of γ-Al_2O_3, while it is promoted by the hydrogen bonding interactions between proximal hydroxyl groups of alumina and water. Since a larger amount of water is present in the reaction system surrounding the catalyst than that adsorbed in the pyridine-FTIR, more remarkable decrease of LAS concentration is expected in the reaction process. As a result, the decrease of the acidity of Pd/Al_2O_3 contributes to the suppression of hydrogenolysis and etherification side reactions.

4. Conclusions

This paper originally reports the application of water-containing system for the highly selective decarbonylation of HMF and investigates the functional mechanism of hydrogen bond of water. The added water as a co-solvent significantly suppressed the side reactions such as dehydrogenation, hydrogenolysis and etherification on hydroxyl group (of HMF or FOL), leading to a high FOL selectivity of 97%. DFT calculations reveal that the hydrogen bonds between hydroxyl groups of FOL and water hinder the dehydrogenation reaction to form FAL and furan. On the other hand, the hydrogen bonds between hydroxyl groups on Al_2O_3 surface and water decrease the acidity of Pd/Al_2O_3 catalyst, and suppress the hydrogenolysis and etherification side reactions.

Appendix A. Supplementary data

Supplementary data associated with this article can be found, in the online version, at http://dx.doi.org/10.1016/j.apcatb.2017.04.069.

References

[1] M. Besson, P. Gallezot, C. Pinel, Chem. Rev. 114 (2014) 1827–1870.
[2] M. Hronec, K. Fulajtarova, T. Liptaj, Appl. Catal. A: Gen. 437 (2012) 104–111.
[3] M. Villaverde, N. Bertero, T. Garetto, A. Marchi, Catal. Today 213 (2013) 87–92.
[4] Q. Yuan, D. Zhang, L. van Haandel, F. Ye, T. Xue, E.J.M. Hensen, Y. Guan, J. Mol. Catal. A: Chem. 406 (2015) 58–64.
[5] K. Fulajtarova, T. Sotak, M. Hronec, I. Vavra, E. Dobrocka, M. Omastova, Appl. Catal. A: Gen. 502 (2015) 78–85.
[6] F.M.A. Geilen, T.V. Stein, B. Engendahl, Sonja Winterle, M.A. Liauw, J. Klankermayer, W. Leitner, Angew. Chem. Int. Ed. 50 (2011) 6831–6834.
[7] Y.B. Huang, Z. Yang, M.Y. Chen, J.J. Dai, Q.X. Guo, Y. Fu, ChemSusChem 6 (2013) 1348–1351.
[8] Q. Meng, C. Qiu, G. Ding, J. Cui, Y. Zhu, Y. Li, Catal. Sci. Technol. 6 (2016) 4377–4388.
[9] Q. Meng, H. Zheng, Y. Zhu, Y. Li, J. Mol. Catal. A: Chem. 421 (2016) 76–82.
[10] Y. Román-Leshkov, M.E. Davis, ACS Catal. 1 (2011) 1566–1580.
[11] C.I. Herrerias, X. Yao, Z. Li, C.J. Li, Chem. Rev. 107 (2007) 2546–2562.
[12] R.N. Butler, A.G. Coyne, Chem. Rev. 110 (2010) 6302–6337.
[13] A. Chanda, V.V. Fokin, Chem. Rev. 109 (2009) 725–748.
[14] J.F. Blake, W.L. Jorgensen, J. Am. Chem. Soc. 113 (1991) 7430–7432.
[15] H. Yoshida, Y. Onodera, S.I. Fujita, H. Kawamori, M. Arai, Green Chem. 17 (2015) 1877–1883.
[16] A. Bhosale, H. Yoshida, S.I. Fujita, M. Arai, Green Chem. 17 (2015) 1299–1307.
[17] G. Kresse, J. Furthmuller, Comp. Mater. Sci. 6 (1996) 15–50.
[18] G. Kresse, J. Furthmuller, Phys. Rev. B 54 (1996) 11169–11186.
[19] P.E. Blochl, Phys. Rev. B 50 (1994) 17953–17979.
[20] G. Kresse, D. Joubert, Phys. Rev. B 59 (1999) 1758–1775.
[21] J.P. Perdew, K. Burke, M. Ernzerhof, Phys. Rev. Lett. 77 (1996) 3865–3868.
[22] S. Grimme, J. Comput. Chem. 27 (2006) 1787–1799.
[23] S. Grimme, J. Antony, S. Ehrlich, H. Krieg, J. Chem. Phys. 132 (2010).
[24] S. Grimme, S. Ehrlich, L. Goerigk, J. Comput. Chem. 32 (2011) 1456–1465.
[25] N.J. Divins, I. Angurell, C. Escudero, V. Perez-Dieste, J. Llorca, Science 346 (2014) 620–623.
[26] K. Mathew, R. Sundararaman, K. Letchworth-Weaver, T.A. Arias, R.G. Hennig, J. Chem. Phys. 140 (2014) 084106.
[27] A. Dias, M. Pillinger, A. Valente, J. Catal. 229 (2005) 414–423.
[28] J. Dai, X. Fu, L. Zhu, J. Tang, X. Guo, C. Hu, ChemCatChem 8 (2016) 1379–1385.
[29] L.D. Lillwitz, US4089871A, 1978.
[30] S. Bhogeswararao, D. Srinivas, J. Catal. 327 (2015) 65–77.
[31] B. Seemala, V. Haritos, A. Tanksale, ChemCatChem 8 (2016) 640–647.
[32] M. Zhang, X. Tong, R. Ma, Y. Li, Catal. Today 264 (2016) 131–135.
[33] J.J. Wang, Z.C. Tan, C.C. Zhu, G. Miao, L.Z. Kong, Y.H. Sun, Green Chem. 18 (2016) 452–460.
[34] P. Wrigstedt, J. Keskiväli, T. Repo, RSC Adv. 6 (2016) 18973–18979.
[35] A. Dibenedetto, M. Aresta, L. di Bitonto, C. Pastore, ChemSusChem 9 (2016) 118–125.
[36] J. Luo, H. Yun, A.V. Mironenko, K. Goulas, J.D. Lee, M. Monai, C. Wang, V. Vorotnikov, C.B. Murray, D.G. Vlachos, P. Fornasiero, R.J. Gorte, ACS Catal. 6 (2016) 4095–4104.
[37] S. Wang, V. Vorotnikov, D.G. Vlachos, ACS Catal. 5 (2015) 104–112.
[38] M. Tatarkhanov, D.F. Ogletree, F. Rose, T. Mitsui, E. Fomin, S. Maier, M. Rose, J. Cerdaí, M. Salmeron, J. Am. Chem. Soc. 131 (2009) 18425–18434.
[39] V. Vorotnikov, G. Mpourmpakis, D.G. Vlachos, ACS Catal. 2 (2012) 2496–2504.
[40] T. Miyazawa, Y. Kusunoki, K. Kunimori, K. Tomishige, J. Catal. 240 (2006) 213–221.
[41] J. Chaminand, L. aurent Djakovitch, P. Gallezot, P. Marion, C. Pinel, C. Rosier, Green Chem. 6 (2004) 359–361.
[42] T. Miyazawa, S. Koso, K. Kunimori, K. Tomishige, Appl. Catal. A: Gen. 329 (2007) 30–35.
[43] I. Gandarias, P.L. Arias, J. Requies, M.B. Güemez, J.L.G. Fierro, Appl. Cata. B: Environ. 97 (2010) 248–256.
[44] R.M. Ravenelle, J.R. Copeland, W.G. Kim, J.C. Crittenden, C. Sievers, ACS Catal. 1 (2011) 552–561.
[45] S. Zhu, Y. Qiu, Y. Zhu, S. Hao, H. Zheng, Y. Li, Catal. Today 212 (2013) 120–126.
[46] A. Corma, M. Renz, Angew. Chem. Int. 119 (2007) 302–304.
[47] H. Firouzabadi, N. Iranpoor, A.A. Jafari, J. Mol. Catal. A: Chem. 227 (2005) 97–100.
[48] J. Datka, A.M. Turek, J.M. Jehng, I.E. Wachs, J. Catal. 135 (1992) 186–199.
[49] C. Morterra, C. Emanuel, G. Cerrato, G. Magnacca, J. Chem. Soc. Faraday Trans. 88 (1992) 339–348.
[50] M. Digne, P. Sautet, P. Raybaud, P. Euzen, H. Toulhoat, J. Catal. 211 (2002) 1–5.
[51] P. Hirva, T.A. Pakkanen, Surf. Sci. 277 (1992) 389–394.
[52] C.X.A. da Silva, V.L.C. Gonçalves, C.J.A. Mota, Green Chem. 11 (2009) 38–41.
[53] R. Gounder, M.E. Davis, J. Catal. 308 (2013) 176–188.
[54] M. Moliner, Y. Roman-Leshkov, M.E. Davis, Proc. Natl. Acad. Sci. U. S. A. 107 (2010) 6164–6168.
[55] E. Nikolla, Y. Romaín-Leshkov, M. Moliner, M.E. Davis, ACS Catal. 1 (2011) 408–410.
[56] P.A. Zapata, J. Faria, M.P. Ruiz, R.E. Jentoft, D.E. Resasco, J. Am. Chem. Soc. (2012) 8570–8578.
[57] M.A. Camblor, A. Corma, S. Iborra, S. Miquel, J. Primo, S. Valencia, J. Catal. 172 (1997) 76–84.
[58] P.Y. Dapsens, C. Mondelli, J. Pérez-Ramírez, ACS Catal. 2 (2012) 1487–1499.